 doi:10.20944/preprints202205.0062.v1

Description of Si and Al Release from Aluminoslicate in the Acidic Condition Using Density Functional Theory: Protonated Terminal Oxygen

Chen-Yang Zhang[1,4], Ya-Ling Yu[1], Huan Yang[1], Li-Ming Wang[2], Ming-Feng Zhong[2], Shao-Min Lin[1,3,*], Zhi-Jie Zhang[2,*], Yun-Ying Wu[4], Wei Xu[2]

[1] School of Materials Science and Engineering, Hanshan Normal University, Chaozhou 521041, China;
[2] School of Materials Science and Engineering, South China University of Technology, Guangzhou; rsqzhao@scut.edu.cn
[3] Chaozhou Branch of Chemistry and Chemical Engineering Guangdong Laboratory;
[4] Guangdong Chaoshan Institute of Higher Education and Technology, Chaozhou 521041, China;
* Correspondence:lsm678@hstc.edu.cn (S. Lin), imzhang@scut.edu.cn (Z. Zhang).

Abstract: The molecular clusters ($(HO)_3Si\text{-}O\text{-}Si(OH)_3$, and $(HO)_3Al\text{-}O\text{-}Si(OH)_3$) representative of aluminosilicate mineral surface were employed to study the dissolution of aluminosilicate in acidic condition via density functional theory (DFT) with the M06-2X+G(d,p) methodology. The surface termination sites (Si and Al) were both tetra-coordinated and the terminal oxygen was protonated in acidic condition. In the dissolution reaction, the calculated barrier height of the six-membered ring transition state complex containing two water molecules was predicted to be lower than that of four-membered ring transition state complex containing one water molecule. In addition, the calculated barrier heights for Al-terminated sites were predicted to be lower than those for the Si-terminated sites, suggesting that breaking the Al-O bond is easier than Si-O bond in the aluminosilicate mineral surface; the barrier heights of the surface termination sites with protonated terminal oxygen were lower than those without protonated terminal oxygen. With the fracture of Si-O and Al-O bonds, the Si and Al release from the aluminosilicate. The result indicates that the acidic condition facilitates the release of Si and Al from the aluminosilicate, and the concentration of Al leaching from aluminosilicate is higher than Si.

Keywords: Aluminosilicate mineral; Dissolution; Protonated terminal oxygen; DFT

1. Introduction

High sintering temperature is required in the porcelain industry as the destruction of Si-O and Al-O bond of aluminosilicate minerals in the raw material need high activation energy[1], which results in high energy consumption. In order to decrease the energy consumption, reduction of the sintering temperature is an effective method. Activating the raw material can destroy the Si-O and Al-O bonds on the mineral surface and then reduce the sintering temperature[2-3]. Acid activation is a common activation method[4-6] since the dissolution rate of mineral increases in acid aqueous solution. Aluminosilicate minerals (such as kaolin and feldspar) account for a large proportion in the raw ceramic material. It is worth investigating the dissolution mechanism of aluminosilicate minerals. A. Steudel[7] has reported that under acidic conditions, the dissolution rate of Si and Al from kaolin and feldspar increased significantly and a large number of Si-O and Al-O bonds in mineral are distructed.

The dissolution of aluminosilicate minerals in the aqueous solution that occurs to some degree nearly everywhere on Earth and has an effect on a number of processes such as soil chemistry, water contaminants, and the global CO_2 cycle. Furthermore, investigating the dissolution mechanisms in acid condition will provide some implication in the acid activation of aluminosilicate minerals. Dissolution of minerals in the aqueous solutions have been studied for nearly a century. Most authors investigated the dissolution rate law of minerals based on the concentration of Si or Al release from minerals[8-10].

Preprints (www.preprints.org) | NOT PEER-REVIEWED | Posted: 6 May 2022 doi:10.20944/preprints202205.0062.v1

However, the hydrolysis of minerals will generally occur in a number of steps rather than as written stoichiometrically. For example, orthoclase dissolution can be described thermodynamically by

$$KAlSi_3O_8 + 4H_3O^+ \rightarrow K^+ + Al^{3+} + 3H_4SiO_4,$$

but the probability of an orthoclase formula unit reacting with $4H_3O^+$ molecules in one step is vanishingly small. Instead, the reaction occurs in a number of elementary steps, such as ion exchange of K^+ , the hydrolysis of individual Al-O-Si and Si-O-Si linkages, the formation of K^+ and Al^{3+} speices. Among these elementary steps, the breakage mechanisms of Al-O and Si-O bonds in the minerals surface have been paid close attention. To investigate the reaction pathways, some scholars have simulated the Si-O and Al-O bond cleavage in the molecular level using quantum mechanical calculations in recent dacades[11-12]. In the paper, the DFT calculations was employed to investigate the hydrolysis reaction of aluminosilicate mineral.

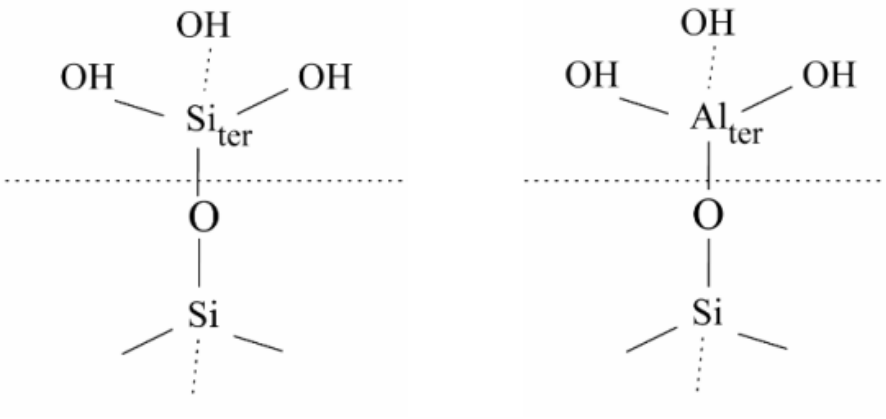

(**a**) (**b**)

Figure 1. Schematic of hydroxylated aluminosilcate mineral surface showing (a) Si and (b) Al terminal.

Three typical molecular clusters (Fig. 1) on aluminosilicate mineral surface is chosen for calculation. The dotted line in Figure 1 represents the surface of the mineral, and each tetra-coordinated Si or Al is terminated with hydroxyl groups. Both the Si and Al terminal sites (Si_{ter} and Al_{ter}) are connected to the bulk of mineral by a bridge oxygen atom. Si sites on the surface is depicted by the Si_{ter}-O-Si to simulate the breakage of Si_{ter}-O bond and the release of Si. Similarly, the Al terminated sites is depicted with Al_{ter}-O-Si to indicate the breakage of Al_{ter}-O bond and the release of Al. The oxygen in the hydroxyl group attached to the Si_{ter} and Alte on the surface is called terminal oxygen.

In the presence of acidic aqueous solution, the H^+ is easy to be captured by the terminal oxygen on hydroxylated aluminosilicate mineral surface for the weak space steric effect. This study focus on the reaction pathway for hydrolyzing Si_{ter}-O-Si and Al_{ter}-O-Si, and the effect of proton on the breakage of Si_{ter}-O and Alter-O bonds. The reaction rate constants was calculated by the Arrheius equation via the barrier height computed by data in the output file. Before the investigation of the barrier height for the Si_{ter}-O-Si and Al_{ter}-O-Si surface sites, the effect of transition state complexes configuration containing four and six membered ring (Fig. 2) on the activation energy is discussed.

Preprints (www.preprints.org) | NOT PEER-REVIEWED | Posted: 6 May 2022 doi:10.20944/preprints202205.0062.v1

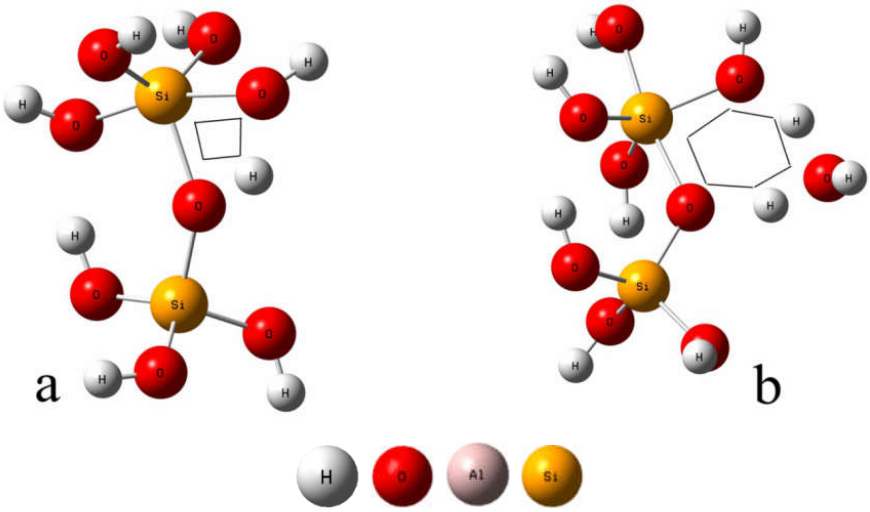

Figure 2. Transition state complexes of Si_{ter}-O-Si reacting with H_2O containing (a) four-membered and (b) six-membered ring.

2. Chemical Reaction

2.1. Reaction Models

The most important aspect of a reaction pathway is determining the transition state complex, which has no stability in time and has no real finite concentration by definition. Recent descriptions of quartz and aluminosilicate mineral dissolution includes different transition state complexes during the hydrolysis of Al-O-Si and Si-O-Si linkage on the mineral surface[13-14]. However, the configurations of the transition state complexes were not discussed. In the paper, the four and six-membered ring transition state complexes for the hydrolysis reaction of aluminosilicate was presented. The four-membered ring configuration contains Si, O atom in the reaction center of Siter-O and H, O from a water molecular (Fig. 2a), whereas the addition of H and O from in the six-membered ring configuration(Fig. 2b) come from another water molecular.

In the beginning of the hydrolysis reaction, the water molecular approached the reaction center and the coordination of Si and Al were changed from four to five. Then the Si_{ter}-O and Al_{ter}-O bonds lengthen and the coordination of Siter and Alter convert into four. At last, the Si and Al species leave away from the mineral surface and migrate to the liquid phase.

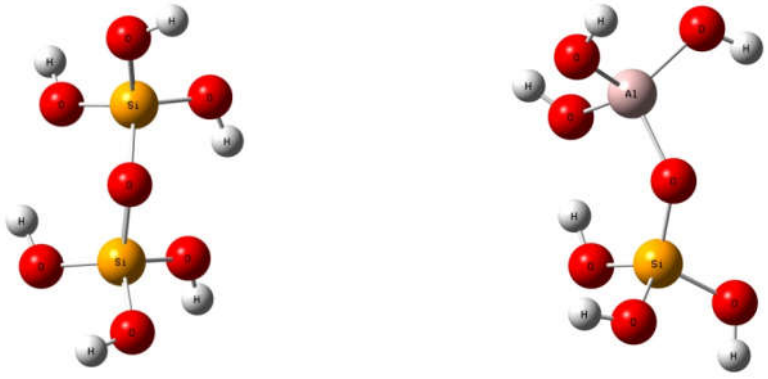

(**a**) (**b**)

Figure 3. The molecular clusters of (a) Si_{ter}-O-Si, and (b) Al_{ter}-O-Si.

Preprints (www.preprints.org) | NOT PEER-REVIEWED | Posted: 6 May 2022 doi:10.20944/preprints202205.0062.v1

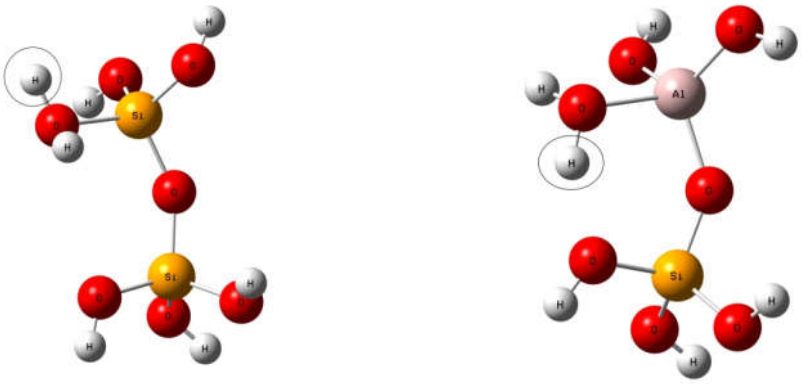

(**a**) (**b**)

Figure 4. The terminal oxygen in (a) Si_{ter}-O-Si and (b) Al_{ter}-O-Si before and after protonation.

To model dissolution process for the surface reaction sites above, the following six reactions were studied. Eqs 1- represent the Si_{ter}-O-Si (Fig. 3a), and Al_{ter}-O-Si (Fig. 4a) sites without protonated terminal oxygen, respectively. With the breakage of Si_{ter}-O or Al_{ter}-O bond, the Si and Al species are extracted from the reaction sites as H_4SiO_4 and $[Al(OH)_4]^-$, respectively. Eqs 3-4 represent the Si_{ter}-O-Si (Fig. 3b), and Al_{ter}-O-Si (Fig. 4b) sites with protonated terminal oxygen, respectively(Fig. 3). After the hydrolysis reaction, the protonated monosilicic acid molecular release from the Siter-O-Si, and the $[Al(OH)_3{\cdot}H_2O]$ forms from the Al_{ter}-O-Si site. The bridge oxygen in the surface sites becomes the terminal oxygen after reaction. The charge of the molecular cluster in the eqs 1-4 is retained during calculation.

$$[(HO)_3Si_{ter}\text{-}O\text{-}Si(OH)_3] + H2O \rightarrow 2Si(OH)_4 \quad (1)$$

$$[(HO)_3Al_{ter}\text{-}O\text{-}Si(OH)_3]^- + H2O \rightarrow [Al(OH)_4]^- + Si(OH)_4 \quad (2)$$

$$[(H_2O)(HO)_2Si_{ter}\text{-}O\text{-}Si(OH)_3]^+ + H2O \rightarrow [Si(OH)_3H_2O]^+ + Si(OH)_4 \quad (3)$$

$$[(H_2O)(HO)_2Al_{ter}\text{-}O\text{-}Si(OH)_3] + H2O \rightarrow [Al(OH)_3H_2O] + Si(OH)_4 \quad (4)$$

2.2. Reaction Rate

Once the reactant and transition state has been optimized in the gas-phase (1 atm, 298 K) for each reaction, the frequency in output files is used to calculate the rate contant via the Arrhenius equation:

$$k = Ae^{\frac{-\Delta E}{RT}}$$

Where A is referred to as the pre-exponential factor, ΔE is the activation energy, R is the gas constant and T is the temperature in degrees Kelvin.

3. Computational Methods

A density functional theory (DFT) is a computational quantum mechanical modelling method that selects the electron density distribution as basic variable to investigate the ground-state properties of multi-particle system. Some articles have applied the DFT method to explain the hydrolysis reaction of the silicate mineral surface successfully[11,15-18]. Thus, the application of the M06-2X functional[19] here to model the hydrolysis of aluminosilicate is reasonable. The employment of the 6-311+G(d,p) basis set is appropriate in this study because the variable coordination number of Si and Al containing d orbitals and p orbitals were added in the case that H is an important factor in

Preprints (www.preprints.org) | NOT PEER-REVIEWED | Posted: 6 May 2022 doi:10.20944/preprints202205.0062.v1

the reaction. All calculations were performed on the reactants, products and transition state complexes given in the eqs 1-6 with Gaussian 09 package[20] without any constrains. The transition state structures are characterized by a single negative frequency.

4. Results

The configurations of transition state complexes were discussed firstly. Then the hydrolysis mechanisms of Siter-O-Si and Alter-O-Si sites in acid condition were investigated.

4.1. The Configuration of Transition State

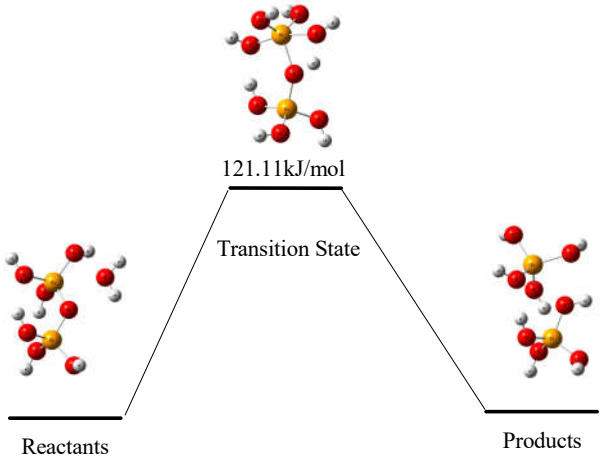

Figure 5. Reaction mechanism for the hydrolsis of the Si_{ter}-O-Si site in the presence of a H_2O molecule. The transition state complex contains a four-membered ring.

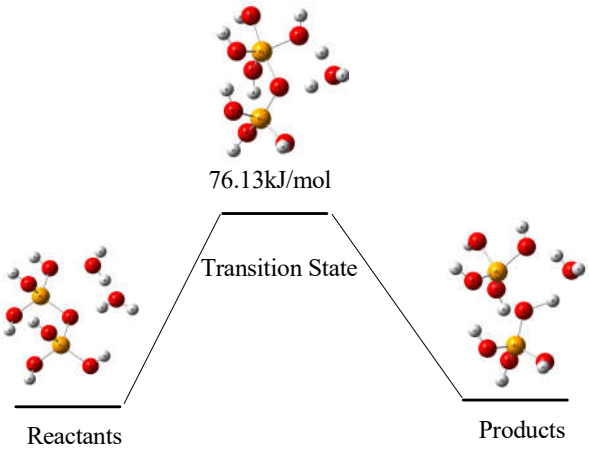

Figure 6. Reaction mechanism for the hydrolysis of the Si_{ter}-O-Si site in the presence of two H_2O molecules. The transition state complex contains a six-membered ring.

The hydrolysis process of Si_{ter}-O-Si with H_2O is shown Fig. 5 and Fig. 6, distinguished by the configuration of transition state complexes. When the Si_{ter}-O-Si surface site reacted with a H_2O molecule (Fig. 5), the transition state complex contained a four-membered ring. Along the reaction path, the H in the water molecule was absorbed by the bridge O and the rest of water molecule (OH) was captured by the Si_{ter}, simultaneously, the Si_{ter}-O bond fractured. The barrier height of this reaction (labelled as R_f) is 121.11 kJ/mol. When the Si_{ter}-O-Si surface site reacted with two H_2O molecules (Fig. 6),

 doi:10.20944/preprints202205.0062.v1

six-membered ring complexes of transition state formed. Along this reaction path, the H in the H_2O beside the bridege O side, bonded with bridge O and the OH in the other H_2O near the Si_{ter}, was captured by the Si_{ter}. In addition, a new water molecule formed by the rest of H and OH from different H_2O molecules, respectively. The barrier height of this reaction (labelled as R_s) is 76.13 kJ/mol.

According the Arrhenius equatioin, the rate constant of R_s is 7.60×10^7 time of the R_f. The lower activation energy and larger rate constant of R_f is possibly attributed to the catalysis by H_2O in the reaction of six membered ring. Compared with the experimental data that the hydrolysis activation energy of quartz, only containing Si-O-Si site, was 67~89 kJ/mol[21-23], the barrier height of six membered ring transition state is reasonable. Thus, the six membered ring configuration of the transition state is appropriate and would be used in the following text.

4.2. Hydrolysis Reaction at Siter-O-Si site

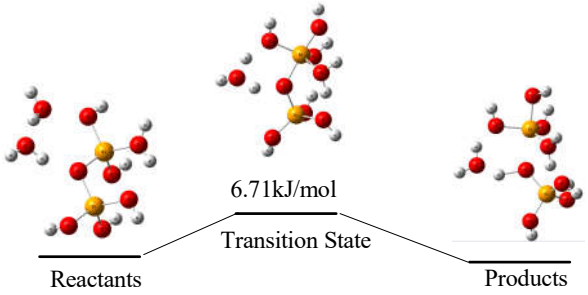

Figure 7. The reaction path of a protonated Si_{ter}-O-Si site.

The energy profiles of Si_{ter}-O-Si with protonated terminal oxygen reacting with two H_2O molecules are shown in Figure 7. After the breakage of the Si_{ter}-O bond on the mineral surface, the Si species was left as $[Si(OH)_3(H_2O)]$. The barrier height of the reaction decreased to 6.17 kJ/mol and is 91.90% lower than that for the Si_{ter}-O-Si without protonation. The rate constant of this hydrolysis reaction is 1.81×10^{12} time of that of the Si_{ter}-O-Si without protonated terminal oxygen. This indicates that the proton facilitates the fracture of Si_{ter}-O bond on the mineral surface, corresponding to the experimental data that the dissolution rate of Si release from quartz and feldspar increases in the acidic condition[24-27].

4.3. Hydrolysis Reaction at Al_{ter}-O-Si site

The energy profiles of hydrolysis reaction at Al_{ter}-O-Si site are shown in Fig. 8. The barrier heights for the Al_{ter}-O-Si without protonation 22.23kJ/mol, respectively. The results suggest that the Al_{ter}-O-Si site is easier to hydrolyze than the Si_{ter}-O-Si site. This maybe attributed to the Si-O bond, which needs higher energy to break.

Fig. 9 shows the energy profile and hydrolysis mechanism of Al_{ter}-O-Si with protonated terminal oxygen. The barrier height is -0.86 kJ/mol. The negative activation energy suggests that a state exists with a lower energy than the transition state. These lead to the same conclusion that the protonated site is easier to hydrolyze than the unprotonated site.

Preprints (www.preprints.org) | NOT PEER-REVIEWED | Posted: 6 May 2022 doi:10.20944/preprints202205.0062.v1

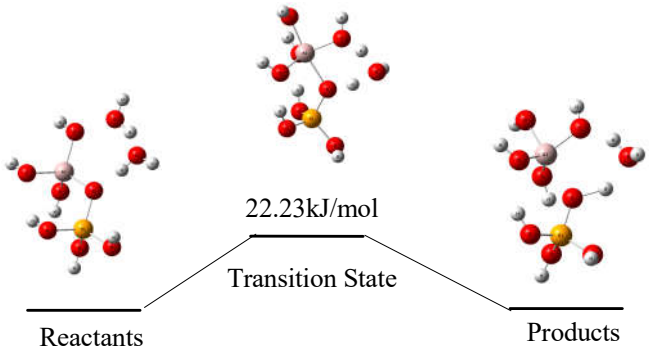

Figure 8. The reaction path of a protonated Al_{ter}-O-Si site without protonated terminal oxygen.

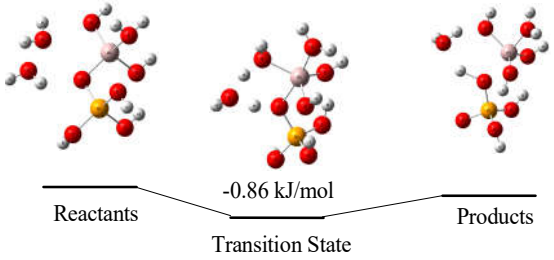

Figure 9. The reaction path of Al_{ter}-O-Si site with protonated terminal oxygen.

Compared to barrier height for the hydrolysis of Si_{ter}-O-Si clusters, the barrier height for the hydrolysis of Al_{ter}-O-Si clusters is lower. This suggests that the Al_{ter}-O-Si site is easier to react with H_2O, which indicates the hydrolysis reaction maybe take place preferentially at the Al_{ter}-O-Si site on the aluminosilicate mineral.

5. Conclusions

The Si_{ter}-O-Si and Al_{ter} -O-Si clusters representative of aluminosilicate mineral surface were employed to study the hydrolysis reactions in acidic condition via density functional theory with the M06-2X+G(d,p) methodology. The transition state complex containing six membered ring for Si_{ter}-O-Si linkage yields barrier heights of 76.13 kJ/mol, which is lower than 121.11 kJ/mol for the complex containing four membered ring and is closer to the experimental data of 67~89 kJ/mol for the hydrolysis activation energy of quartz.

In the hydrolysis reaction, the calculated barrier heights of Si_{ter}-O-Si and Al_{ter}-O-Si clusters without protonated terminal oxygen molecular are 76.13, 22.23 kJ/mol, respectively; the calculated barrier heights of Si_{ter}-O-Si, and Al_{ter}-O-Si clusters with protonated terminal oxygen molecular are 6.71, and -0.86 kJ/mol. It is obvious that the barrier height decreased as the terminal oxygen was protonated and the hydrolysis activation energy of Al_{ter}-O was lower than that of Si_{ter}-O before and after protonation. The barrier height of the three surface sites is ranged as: Al_{ter}-O-Si < Si_{ter}-O-Si. With the fracture of Si_{ter}-O and Al_{ter}-O bond, the Si and Al are released from the aluminosilicate. These results confirm that proton facilitates the release of Si and Al, and the dissolution of Al is easier than Si in the aluminosilicate mineral surface.

Author Contributions: Conceptualization, Chen-Yang Zhang; methodology, Huang Yang; software, Li-Ming Wang; validation, Ya-Ling Yu; formal analysis, Ming-Feng Zhong; investigation, Ya-Ling Yu; resources, Huang Yang and Wei Xu; data curation, Yun-Ying Wu; writing—original draft preparation, Chen-Yang Zhang, Shao-Min Lin; writing—review and editing, Chen-Yang Zhang and Li-Ming Wang; visualization, Zhi-Jie Zhang; supervision, Shao-Min Lin; project ad-

ministration, Shao-Min Lin and; funding acquisition, Ya-Ling Yu, and Zhi-Jie Zhang. All authors have read and agreed to the published version of the manuscript.

Funding: This research was funded by the National Natural Science Foundation of China (Nos. 21207027 and 51372090), the Hanshan Normal University Scientific Research Foundation (No. XN201919), and the Chaozhou Science and Technology Planning Project (No. 2021ZC29).

Data Availability Statement: Not applicable.

Acknowledgments: Advanced ceramic innovation research center of Hanshan Normal University, Chaozhou Branch of Chemistry and Chemical Engineering Guangdong Laboratory, and Guangdong Chaoshan Institute of Higher Education and Technology are all acknowledged.

Conflicts of Interest: The authors declare no conflict of interest. The funders had no role in the design of the study; in the collection, analyses, or interpretation of data; in the writing of the manuscript, or in the decision to publish the results.

References

1. Huggins M.L.; Sun K.-H. Energy Additivity in Oxygen-containing Crystals and Glasses. J. Phys. Chem., 1946, 50(4), 319–328.
2. Lin S., Yu Y., Zhong M., Yang H., Zhang C., Zhang, Z.; Xu W., Xie J., Qiu Y.. The activation mechanism of oxalic acid on γ-alumina and the formation of α-alumina. Ceramics International, 2021,47, 26869-26876.
3. Zhang, C.; Zhang, Z.; Tan, Y.; Zhong, M.. The Effect of Citric Acid on the Kaolin Activation and Mullite Formation. Ceramic International, 2017, 43, 1466-1471.
4. Czech K., Banaś D., Kubala-Kukuś, A., Stabrawa, I.. The effect of chemical modification on the physico-chemical characteristics of halloysite : FTIR, XRF, and XRD studies. Journal of Molecular Structure, 2015, 1084:16-22.
5. Chaar,i I., Medhioub, M., Jamoussi, F., Hamzaoui, A.H.. Acid-treated clay materials (Southwestern Tunisia) for removing sodium leuco-vat dye : Characterization, adsorption study and activation mechanism. Journal of Molecular Structure, 2020, 1223:128944.
6. Lin, S.L., Yu, Y.L., Zhang, Z.J., Zhang, C.Y., Zhong, M.F., Wang. L.M., Lu, S.X., Xu W., Li, N., Huang, X.. The synergistic mechanisms of citric acid and oxalic acid on the rapid dissolution of kaolinite. Applied Clay Science, 2020, 196: 105756.
7. Steudel, A.; Batenburg, L.F.; Fischer, H.R.; Weidler, P.G.; Emmerich, K. Alteration of Non-Swelling Clay Minerals and Magadiite by Acid Activation. Applied Clay Science, 2009, 44, 95-104.
8. Zhang C., Zhang Y., Rimstidt J. D., Gong L., BurkhartJ.A.C., Chen K., Yuan H.. Testing hypotheses of albite dissolution mechanisms at near-equilibrium using Si isotope tracers. Geochimica et Cosmochimica Acta, 2021, 303, 15-37.
9. J. Cama and J. Ganor, The Effects of Organic Acids on the Dissolution of Silicate Minerals - A Case Study of Oxalate Catalysis of Kaolinite Dissolution. Geochimica et Cosmochimica Acta, 2006, 70, 2191–2209.
10. Che Z., Nightingale M., Tutolo Benjamin M.. Probing the application of kinetic theory to Mg-phyllosilicate growth with Si isotope doping, Geochimica et Cosmochimica Acta, 2021, 310, 205-220.
11. Shikha, N.; Barbara, J.G. Reaction Rates and Dissolution Mechanisms of Quartz as a Function of pH. J. Phys. Chem.A, 2008, 112, 2027-2033.
12. Inna, K.; Andreas, L. Kinetic Monte Carlo Simulations of Silicate Dissolution: Model Complexity and Parametrization. J. Phys. Chem. A, 2013, 117, 24894–24906.
13. Zhang, Y., Rimstidt, D.J., Huang, Y. Zhu C.. Kyanite far from equilibrium dissolution rate at 0–22 °C and pH of 3.5–7.5. Acta Geochim, 2019, 38, 472–480.
14. Yokoyama T., Nishiyama N.. Dissolution of Minerals Driven by the Wetting Film in Rock Pores: Comparison of Silicates and Carbonates. ACS Earth Space Chem, 2020, 4, 11, 1920-1930
15. Schliemann R., Churakov S., Pyrophyllite dissolution at elevated pressure conditions: An ab initio study. Geochimica et Cosmochimica Acta, 2021, 307, 42-55.
16. Fu R., Shen X., Lacks D., First-Principles Study of the Charge Distributions in Water Confined between Dissimilar Surfaces and Implications in Regard to Contact Electrification, J. Phys. Chem. C, 2017, 121, 22, 12345–12349.
17. Wang, X.; Zhang, Q.; Li, X.; Ye, J.; Li, L. Structural and Electronic Properties of Different Terminations for Quartz (001) Surfaces as Well as Water Molecule Adsorption on It: A First-Principles Study. Minerals 2018, 8, 58.
18. Felipe A., Kubicki D., Rye M.. Hydrogen isotope exchange kinetics between H_2O and H_4SiO_4 from ab initio calculations. Geochimica et Cosmochimica Acta, 2003, 67, 1259-1276.
19. Zhao, Y.; Truhlar, D. G. The M06 Suite of Density Functionals for Main Group Thermochemistry, Thermochemical Kinetics, Noncovalent Interactions, Excited States, and Transition Elements: Two New Functionals and Systematic Testing of Four M06-class Functionals and 12 Other Functionals. Theor. Chem. Acc., 2008, 120, 215-241.
20. Frisch, M.J., Trucks, G.W., Schlegel, H.B., Scuseria, G.E., Robb, M.A., Cheeseman, J.R., Scalmani, G., Barone, V., Mennucci, B., Petersson, G.A., Nakatsuji, H., Caricato, M., Li, X., Hratchian, H.P., Izmaylov, A.F., Bloino, J., Zheng, G., Sonnenberg, J.L., Hada, M., Ehara, M., Toyota, K., Fukuda, R., Hasegawa, J., Ishida, M., Nakajima, T., Honda, Y., Kitao, O., Nakai, H., Vreven, T., Montgomery Jr., J.A., Peralta, J.E., Ogliaro, F., Bearpark, M., Heyd, J.J., Brothers, E., Kudin, K.N., Staroverov, V.N., Kobayashi, R., Normand, J., Raghavachari, K., Rendell, A., Burant, J.C., Iyengar, S.S., Tomasi, J., Cossi, M., Rega, N., Millam, J.M., Klene,

M., Knox, J.E., Cross, J.B., Bakken, V., Adamo, C., Jaramillo, J., Gomperts, R., Stratmann, R.E., Yazyev, O., Austin, A.J., Cammi, R., Pomelli, C., Ochterski, J.W., Martin, R.L., Morokuma, K., Zakrzewski, V.G., Voth, G.A., Salvador, P., Dannenberg, J.J., Dapprich, S., Daniels, A.D., Farkas, O., Foresman, J.B., Ortiz, J.V., Cioslowski, J. and Fox, D.J. (2009) Gaussian 09, Revision D.01. Gaussian, Inc., Wallingford.

21. Casey, W.H.; Lasaga, A.C.; Gibbs, G.V. Mechanisms of Silica Dissolution as Inferred From the Kinetic Isotope Effect. 1990, 12, 3369-3378.
22. Polster, W.; Barnes, H.L. Kinetics of Quartz Precipitation and Dissolution under Hydrothermal Conditions at 100 to 300°C. Geological Society of America, 1992,24:7.
23. Bird, G.; Boon, J.; Stone, T. Silica Transport during Steam Injection into Oil Sands: 1. Dissolution and Precipitation Kinetics of Quartz: New Results and Review of Existing Data. Chemical Geology, 1986, 54, 69-80.
24. Welch, S.A.; Ullman, W.J. Feldspar Dissolution in Acidic and Organic Solutions: Compositional and pH Dependence of Dissolution Rate. Geochimica et Cosmochimica Acta, 1996. 60, 2939-2948.
25. Steudel, A.; Batenburg, L.F.; Fischer, H.R.; Weidler, P.G.; Emmerich, K. Alteration of Swelling Clay Minerals and Magadiite by Acid Activation. Applied Clay Science 44. Applied Clay Science, 2009, 44, 105-115.
26. Lange I., Toro M., Arvidson R., Kurganskaya I., Luttge A.. The role of crystal heterogeneity in alkali feldspar dissolution kinetics, Geochimica et Cosmochimica Acta, 2021, 309, 329-351.
27. Zhu C., Rimstidt J., Zhang Y.,Kang J., Schott J., Yuan H.. Decoupling feldspar dissolution and precipitation rates at near-equilibrium with Si isotope tracers: Implications for modeling silicate weathering, Geochimica et Cosmochimica Acta, 2020, 271, 132-153.